NITRIDING OF HIGH SPEED STEEL[1]

E.D. Doyle[2]
A.M. Pagon[2]
P. Hubbard[2]
S.J. Dowey[2]
A. Pilkington[2]
D.G. McCulloch[2]
K. Latham[2]
J. DuPlessis[2]

Abstract
Current practice when nitriding HSS cutting tools is to avoid embrittlement of the cutting edge by limiting the depth of the diffusion zone. This is accomplished by reducing the nitriding time and temperature and eliminating any compound layer formation. However, in many applications there is an argument for generating a compound layer with beneficial tribological properties. In this investigation results are presented of a metallographic, XRD and XPS analysis of nitrided surface layers generated using active screen plasma nitriding and reactive vapour deposition using cathodic arc. These results are discussed in the context of built up edge formation observed while machining inside a scanning electron microscope.
Keywords: Nitriding; High speed steel; Machining.

[1] *Technical contribution to the 18th IFHTSE Congress - International Federation for Heat Treatment and Surface Engineering, 2010 July 26-30th, Rio de Janeiro, RJ, Brazil.*
[2] *RMIT University, Melbourne, Victoria, Australia.*

1 INTRODUCTION

Nitriding is a well established diffusion-based thermo-chemical surface treatment used widely throughout industry. The primary objective, in most applications, is one of increasing surface hardness to improve wear resistance. Additional benefits accrue depending on the process parameters selected. For example, improved fatigue resistance, due to the generation of high compressive residual stresses,[1] improved corrosion resistance due to the generation of a dense compound layer[2] and improved resistance to sliding wear due to the formation of an oil retaining porous compound layer.[3] The performance benefits to be gained from nitriding depend on the structure of the nitrided surface. At the outermost surface is the so-called compound layer which is basically iron nitride (γ'-Fe4N and/or ε-Fe2-3N). Beneath this is the diffusion zone that forms as a result of precipitation of fine scale alloy nitrides. The properties of the diffusion zone are a function of the alloying elements present in solution in the steel. In general, the higher the alloy content of the steel, the greater the solubility of nitrogen but the lower the nitrogen activity coefficient.[4] Consequently, the expectation when nitriding very high alloy steels, such as high speed steel (HSS), is for high levels of surface hardness and reduced depths of hardening.

Unfortunately, very high values of surface hardness are invariably attained at the cost of reduced fracture toughness resulting in embrittlement. In the case of HSS this is particularly relevant given that the major application for HSS is in cutting tools. This danger is well recognized by industry, so much so, that nitriding times for HSS are kept very low of the order of tens of minutes rather than hours, as is the case for nitriding of low-alloy alloy steels. Also, nitriding temperatures are kept below 500°C.

In the case of nitriding of cutting tools the problem of embrittlement is further compounded by their complex geometry. Kwietniewski et al.[5] recently observed a higher uptake of nitrogen around the cutting edge which gave rise to deeper diffusion zone with consequent danger of embrittlement and poor tool life due to edge chipping. In the opinion of Kwietniewski et al., this problem is enhanced in plasma-nitriding because of the higher plasma current density at the cutting edge and, therefore, locally higher nitriding temperatures. In addition, it is well recognized[6] that a partial or complete decarburization takes place in the diffusion zone. Some of the carbon diffuses to the surface while some diffuses inwards. Nayal et al.[6] have shown clearly that this can result in the formation of ion carbide (Fe_3C) networks at the grain boundaries, leading to further embrittlement problems resulting in edge chipping.

The commercial practice then of nitriding HSS is one in which nitriding depth profiles are kept shallow in order to avoid problems of embrittlement and the compound layer is avoided. However, Smith and Gane[7] pointed out that, in addition to surface hardening, there is a possible second aim when nitriding HSS cutting tools, that is, to reduce the tendency of the work material to weld and pick up on the cutting edge. This, they maintain, is an issue when drilling or tapping into low carbon, low alloy steel workpieces.

Consequently, when nitriding HSS cutting tools, there may be a further requirement, in addition to surface hardening, to reduce friction at the chip/tool interface. One might therefore consider the potential benefits of generating a tribologically beneficial compound layer. Indeed, this is the principle that underpins the practice of nitrocarburising in which process parameters are selected to favour the development of a compound consisting largely of ε-$Fe_{2\text{-}3}CN$.

In this paper, we report preliminary findings of an investigation into structure and composition of nitrided layers generated under three conditions: the first, active screen plasma nitriding (ASPN) for short times at a low nitriding temperature (480°C). The second, ASPN at high nitriding temperature (570°C) and third, reactively vapour depositing HSS in a nitrogen atmosphere using cathodic arc technology. This work is presented in the context of generating low friction compound layers while limiting the growth of a potentially embrittling diffusion zone and reducing the extent of pick up at the cutting edge. Insight into the latter is presented using images obtained from machining inside a scanning electron microscope.

2 EXPERIMENTAL

2.1 Materials

Two nitriding processes were used in this study. The first was ASPN and the second physical vapour deposition of HSS using a cathodic arc in a nitrogen atmosphere.

2.1.1. M2 HSS treated by ASPN

Before treatment by ASPN, two M2 HSS coupons were polished to a mirror finish using diamond polishing pads. The first sample (ASPN1) was heated in an H_2 atmosphere to a temperature of 480° C and nitrided in an atmosphere of 70%H/30%N for 30 minutes. The second sample (ASPN2) was heated in an H_2 atmosphere to a temperature of 570°C and nitrided in an atmosphere of 65%H/25%N/10%CH_4 for 30 minutes. A reference sample of pure iron (ASPNFe) was included in this second experiment. The ASPN system used here has been previously described by Hubbard et. al.[8]

2.1.2. Film prepared by PVD

Using cathodic arc technology, a thin film of HSS (HSS film) was reactively deposited with nitrogen from an M2 HSS cathode onto silicon wafers. The silicon wafers were argon ion etched before deposition. Nitrogen was introduced into the chamber to a pressure of 2Pa. HSS was reactively deposited with the silicon wafers positioned directly in front of the cathode. The substrate bias voltage was set at 100V.

2.2 Sample Analysis

The ASPN treated HSS coupons were cut, mounted in cross section and polished to a mirror finish using diamond polishing pads before etching in nital (4%). The cross sectional metallography was then studied using a FEI Nova Nano SEM fitted with a backscatter electron detector.

The structure of the nitrided samples was determined using x-ray diffraction (XRD). This was performed using a Bruker AXS D8 ADVANCE wide-angle x-ray diffractometer using graphite-monochromated Cu K_α radiation (λ=1.5406 Å) with a potential of 40 kV and a current of 35 mA: scan range 10-90° 2θ, step size 0.02° and a count rate of 2 seconds.

X-ray photoelectron spectroscopy (XPS) spectra were recorded using a Thermo Scientific K-Alpha XPS. XPS depth profiling was performed and peaks were fitted using the Avantage data spectrum processing software package.

3 RESULTS AND DISCUSSION

Results from the metallographic examination of the diffusion treated samples are shown in Figure 1. Figure 1(a) shows that it is difficult to resolve any change in the optical microstructure ASPN1. In contrast, Figure 1(b) shows evidence of nitriding in ASPN2 in the form of a well developed acicular structure extending some 30 μm below the surface. A metallographic analysis of the HSS film on silicon was not conducted.

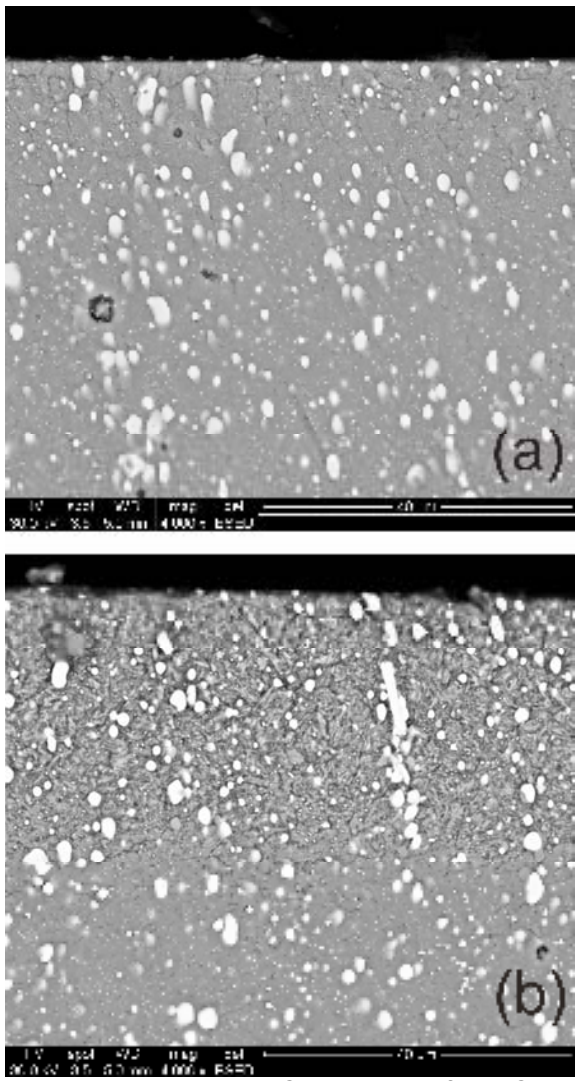

Figure 1. Metallographic cross- sectional SEM images of (a) ASPN1 and (b) ASPN2.

X-ray diffraction was conducted on ASPN1, ASPN2 and the HSS film on silicon as shown in Figure 2. Figure 2(a) is the X-ray diffractogram for ASPN1. It is evident that all X-ray lines can be indexed to the primary HSS carbides (M_6C and MC) and body-centered cubic α- iron. No X-ray lines could be unambiguously assigned to any of the iron nitrides. Figures 2(b) is the X-ray diffractogram for ASPN2. Again most of the X-ray lines can be indexed to the primary carbides (M_6C and MC) and body-centered cubic α-iron. However there are two X-ray lines at a 2θ angle of 41.3° which can be indexed to $\varepsilon + \gamma'$ and another line at 48° which can be indexed to γ'.

Since no other lines can be indexed to ε, we conclude that this nitrided sample is a mixture of iron and iron nitride (γ′), with no compound layer present. Notwithstanding the introduction of methane into the nitriding chamber during nitriding ε iron nitride was not observed. This may be due to the relatively low nitriding potential used in this treatment. The X-ray diffractogram shown in Figure 2(c) for the HSS film is different from the other two diffractograms. The X-ray lines are much broader, probably a result of the much finer grain structure in the HSS film. The body-centered cubic α-iron lines can be indexed while the primary carbides are less clearly defined. There are, however, three X-ray lines which can be indexed to the hexagonal ε iron nitride phase as indexed in Figure 2(c).

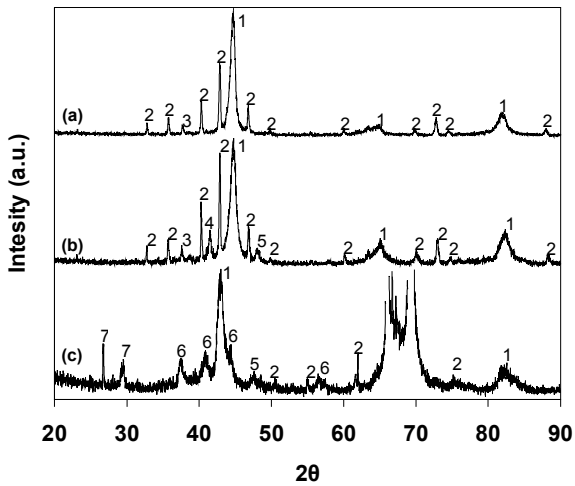

Figure 2. XRD diffractograms of (a) ASPN1 (b) ASPN2 and (c) HSS film. The peaks have been indexed accordingly; 1= body-centered cubic α-iron, 2= M_6C, 3= VC, 4= ε + γ′, 5= γ′, 6= ε, 7= $M_{23}C_6$.

The XPS results for the as received M2, ASPN1, ASPN2, HSS film and ASPNFe are presented in two forms. The first form is the average values of the elements present in the sub-surface. It should be noted that the sub-surface profiles for all the elements showed little variation up to a depth of ~1μm, hence only average values are shown in Table 1. The second is in the form of XPS spectra for the N1s peaks for all the nitrided surfaces.

Table 1. Average elemental concentrations (at%) for each sample

	Fe	N	Cr	O	W	Mo	V	C
M2	73.3	-	3.1	9.5	4.2	3.9	1.5	5.0
ASPN Fe	87.8	10.3	-	1.9	-	-	-	-
ASPN 1	76.8	1.7	2.9	6.2	3.6	3.4	1.5	3.9
ASPN 2	75.5	4.7	2.8	5.8	3.6	3.3	1.7	2.7
HSS Film	72.5	15.1	3.3	2.9	2.2	2.3	1.1	0.5

Table 1 shows average elemental concentrations in atomic percent for each of the samples including the as-received M2 HSS and ASPNFe. The as-received HSS sample is included in the study as an internal reference. The elemental concentrations do fully agree with the supplier specifications for M2 HSS. This is not unexpected given the fact that the sample was sputtered in order to obtain the depth profile. In a sample such as HSS it is inevitable that there will be some preferential

sputtering, particularly in relation to the primary carbides, which directly affects the sensitivity factors in the estimation of the elemental concentrations. Notwithstanding this, it is evident from Table 1, for example, that not all elements are successfully transferred, in the same concentration levels, from the cathode to vapour deposited film. Also, there appears to be some decarburisation of sample ASPN2 that is consistent with the findings of other workers.

With respect to the nitrogen concentrations, there is an interesting trend. In ASPN1 there is a very low uptake of nitrogen that is consistent with the metallographic cross section analysis and the XRD. There is clearly more nitrogen in ASPN2, sufficient enough to record the presence of γ' Fe_4N and be resolvable optically in metallographic cross- section. The ASPNFe sample, nitrided in the same cycle as ASPN2, appears to have double the uptake of nitrogen. This again is consistent with the findings of Somers and Mittemeijer[4] in their studies of nitriding of pure iron. The HSS Film sample shows a high level of nitrogen uptake. This again is consistent with finding ε-iron nitride in the XRD analysis.

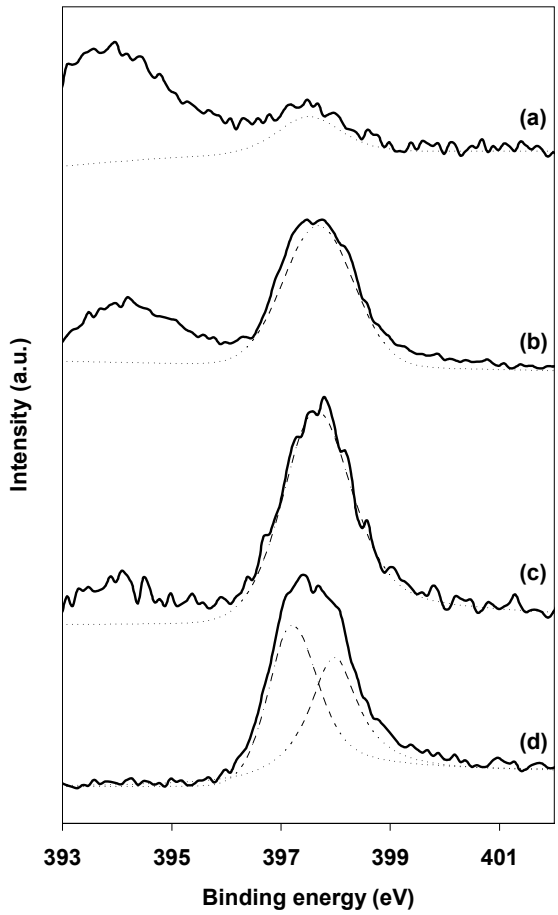

Figure 3. Normalised N1s spectra of (a) ASPN1, (b) ASPN2, (c) HSS Film and (d) ASPNFe. The spectra are not corrected for charging effects. The additional peak in (a), (b) and (c) at ~394 eV is a Mo peak.

The N1s spectra are shown in Figure 3 for (a) ASPN1, (b) ASPN2, (c) HSS Film and (d) ASPNFe. The line shape of the N1s spectrum for ASPNFe suggests the presence of two peaks at binding energies of 397.2 eV and 297.8 eV. We assume

that these two peaks could be assigned to the two forms of iron nitride, namely γ'-Fe_4N and ε-$Fe_{2\text{-}3}N$. It is less clear that one can assign two peaks to the N1s spectrum data shown in Figure 3(c). However, from XRD analysis, we know that the HSS film contains ε and most likely γ'. In contrast, we know from the XRD analysis that ASPN2 contains only γ' and so it is unlikely that two peaks could be fitted to the spectrum as seen in Figure 3(b). It is evident from Figure 3(a) that the spectrum of ASPN1 indicates the presence of iron nitride although it was not detected in both the XRD and metallographic analysis.

The final part of this investigation addresses the issue of "pick-up" or material transfer as raised by Smith and Gane.[7] This relates directly to the friction occurring at the chip/cutting tool interface in the immediate vicinity of the cutting edge, particularly when machining low carbon, low alloy steels at moderate cutting speeds. It also focuses on the nature of separation within the workpiece material at the cutting edge. The latter is an issue of renewed research interest through the recent work of Atkins and colleagues.[9-10] Some insight into the nature of metallurgical processes occurring around the cutting edge can be gained by observing the cutting process directly by machining inside the scanning electron microscope (SEM). One of the present authors conducted such a study and selected images of chip formation in mild steel are shown in Figure 4. Figure 4(a) shows that at the start of the cutting process a so-called continuous chip is formed. Within a short period of time, this gives way to built-up edge (BUE) formation, see Figure 4(b). This is a well known phenomenon and is a consequence of the high friction conditions at the chip/rake face interface. The dynamics of BUE formation are such that the BUE grows in size, becomes unstable and breaks away from the cutting tool. From then on a repeating pattern is established of BUE formation, growth, breakdown and regeneration. Figure 4(c) captures the BUE as it breaks down. It is evident that fracture of the BUE results in the clearance face of the cutting tool being unsupported and hence can lead to edge chipping, particularly, if the cutting edge is embrittled in the nitriding process. If the cutting tool has sufficient fracture toughness to survive this complex loading it may wear rapidly as a result of adhesive wear processes.

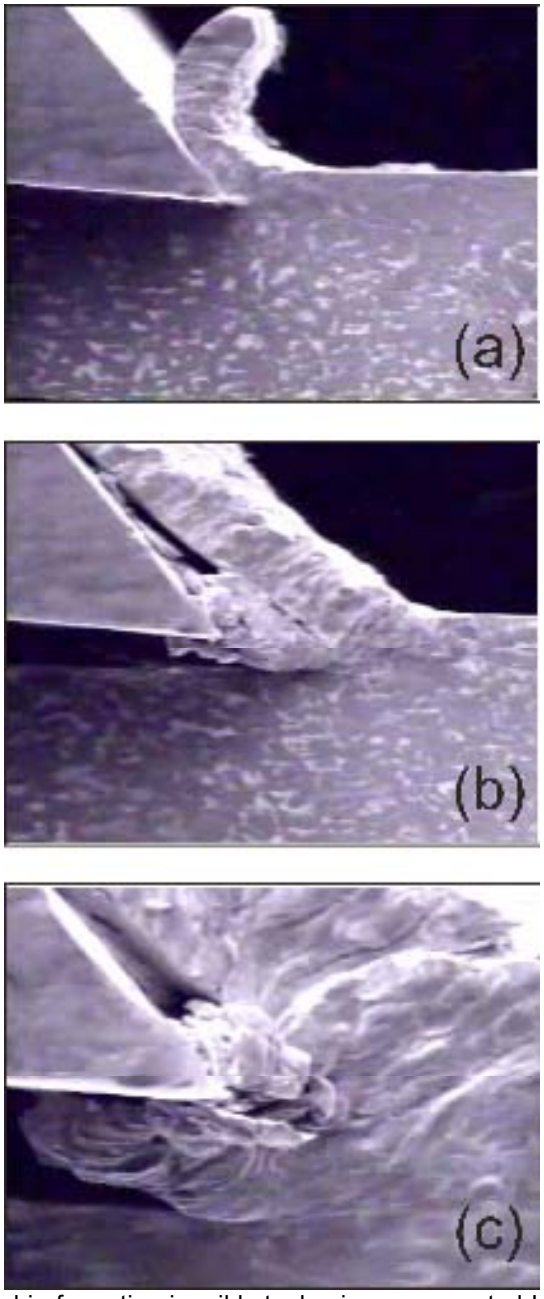

Figure 4. SEM images of chip formation in mild steel using an uncoated HSS cutting tool. (a) shows continuous chip formation at the start of cutting, (b) shows the development of a BUE and (c) shows the break down of the BUE.

4 CONCLUDING REMARKS

When nitriding HSS for cutting tool applications, it is evident that there is potential benefit in generating a compound layer with low friction tribological properties, in addition to a hard fracture tough diffusion zone. In this preliminary study, the ASPN nitriding conditions selected where of too low a nitriding potential to allow the generation of a largely ε iron nitride layer. Further studies will be conducted using a higher nitriding potential while at the same time limiting the growth of the diffusion zone. Interestingly, the vapour deposition of HSS holds promise for generating high hardness combined with improved tribological properties as a result of the formation

of ε iron nitride along with a fine grained ferritic structure. However there are difficulties associated with arc deposition from a ferromagnetic cathode.

Acknowledgements

The authors would like to acknowledge the technical and financial support given to this project by the Chief Executive Officer and directors of Sutton Tools Pty. Ltd. The authors also wish to acknowledge the support of the Australian Research Council and the Defence Materials Technology Centre.

REFERENCES

1 A. Da Silva Rocha, T. Strohaecker, V. Tomala, T. Hirsch, Surf. Coat. Technol., 115 (1) (1999) 24-31.
2 F.Z. Bouanis, F. Bentiss, M. Traisnel, C. Jama, Electrochimica Acta, 54 (8) (2009) 2371-2378.
3 T. Bell, Heat Treatment of Metals, 2 (2) (1975) 39-49.
4 M.A.J. Somers, E.J. Mittemeijer, Surface Engineering, 3 (2) (1987) 123-37.
5 C. Kwietniewski, W. Fontana, C. Moraes, A. da S Rocha, T. Hirsch, A. Reguly, Surface & Coatings Technology, 179 (1) (2004) 27-32.
6 G. Nayal, D.B. Lewis, M. Lembke, W.D. Munz, J.E. Cockrem, Surf. Coat. Technol., 111 (2-3) (1999) 148-157.
7 A.P. Smith, N. Gane, National Conference Publication - Institution of Engineers, Australia, (1977) 207-210.
8 P. Hubbard, J.G. Partridge, E.D. Doyle, D.G. McCulloch, M.B. Taylor, S.J. Dowey, Surf. Coat. Technol., 204 (8) 1145-1150.
9 A.G. Atkins, Inter. J. Mech. Sci., 45 (2) (2003) 373-396.
10 P.A.R. Rosa, O. Kolednik, P.A.F. Martins, A.G. Atkins, Int. J. Mach. Tools Manuf., 47 (12-13) (2007) 1904-1915.